

Effects of uniform extracellular DC electric fields on excitability in rat hippocampal slices *in vitro*

Marom Bikson¹, Masashi Inoue², Hiroki Akiyama², Jackie K. Deans¹, John E. Fox¹, Hiroyoshi Miyakawa² and John G. R. Jefferys¹

¹Department of Neurophysiology, University of Birmingham, Birmingham, UK

²Department of Life Science, Tokyo University of Pharmacy and Life Science, Tokyo, Japan

The effects of uniform steady state (DC) extracellular electric fields on neuronal excitability were characterized in rat hippocampal slices using field, intracellular and voltage-sensitive dye recordings. Small electric fields ($<|40|$ mV mm⁻¹), applied parallel to the somato-dendritic axis, induced polarization of CA1 pyramidal cells; the relationship between applied field and induced polarization was linear (0.12 ± 0.05 mV per mV mm⁻¹ average sensitivity at the soma). The peak amplitude and time constant (15–70 ms) of membrane polarization varied along the axis of neurons with the maximal polarization observed at the tips of basal and apical dendrites. The polarization was biphasic in the mid-apical dendrites; there was a time-dependent shift in the polarity reversal site. DC fields altered the thresholds of action potentials evoked by orthodromic stimulation, and shifted their initiation site along the apical dendrites. Large electric fields could trigger neuronal firing and epileptiform activity, and induce long-term (>1 s) changes in neuronal excitability. Electric fields perpendicular to the apical–dendritic axis did not induce somatic polarization, but did modulate orthodromic responses, indicating an effect on afferents. These results demonstrate that DC fields can modulate neuronal excitability in a time-dependent manner, with no clear threshold, as a result of interactions between neuronal compartments, the non-linear properties of the cell membrane, and effects on afferents.

(Received 25 September 2003; accepted after revision 16 February 2004; first published online 20 February 2004)

Corresponding author J. G. R. Jefferys: Division of Neuroscience (Neurophysiology), University of Birmingham School of Medicine, Edgbaston, Birmingham B15 2TT, UK. Email: j.g.r.jefferys@bham.ac.uk

Application of weak extracellular DC electric fields modulates neuronal activity. They can be used to study normal neuronal (Jefferys, 1981; Richardson *et al.* 1984; Bawin *et al.* 1986; Chan & Nicholson, 1986; Chan *et al.* 1988; Wong & Stewart, 1992; Jefferys, 1995; Andreasen & Nedergaard, 1996) and cognitive function (Nitsche & Paulus, 2000; Walsh & Cowey, 2000; Liebetanz *et al.* 2002). Applied electric fields have clinical applications (Gluckman *et al.* 1996; Ghai *et al.* 2000; Benabid *et al.* 2000; Grill & Kirsch, 2000; Durand & Bikson, 2001), while the potential risks of exposure to environmental electromagnetic fields remain an area of concern (Freude *et al.* 1998; Saunders & Jefferys, 2002).

The purpose of the present report was to test the following hypotheses: (1) the polarity and degree of cell polarization is a function of the dendritic morphology and orientation relative to the applied DC field; (2) the effect of DC fields on excitability is mediated by soma polarization; (3) the efficacy of applied DC fields is time invariant; and (4) DC fields have no effect once the stimulation is ended.

The sources of deviations from the above hypotheses are analysed and implications for environmental and clinical applications are considered.

We characterized the effects of uniform extracellular DC electric fields on rat hippocampal function *in vitro* using field, intracellular and voltage-sensitive dye recordings. These approaches provide the first detailed spatio-temporal map of neuronal polarization, demonstrating differences in the peak and time constant of polarization along the neuron axis. Our results show that dendritic depolarization can increase neuronal excitability (even during somatic hyperpolarization) and that electric fields could shift the action potential initiation zone along the apical dendrite. Moreover, we show that DC electric fields can also affect afferents to CA1 and thus modulate excitability at all field orientations. Large DC electric fields could also modulate neuronal activity in a highly non-linear manner leading to short and long-term changes in excitability and network function.

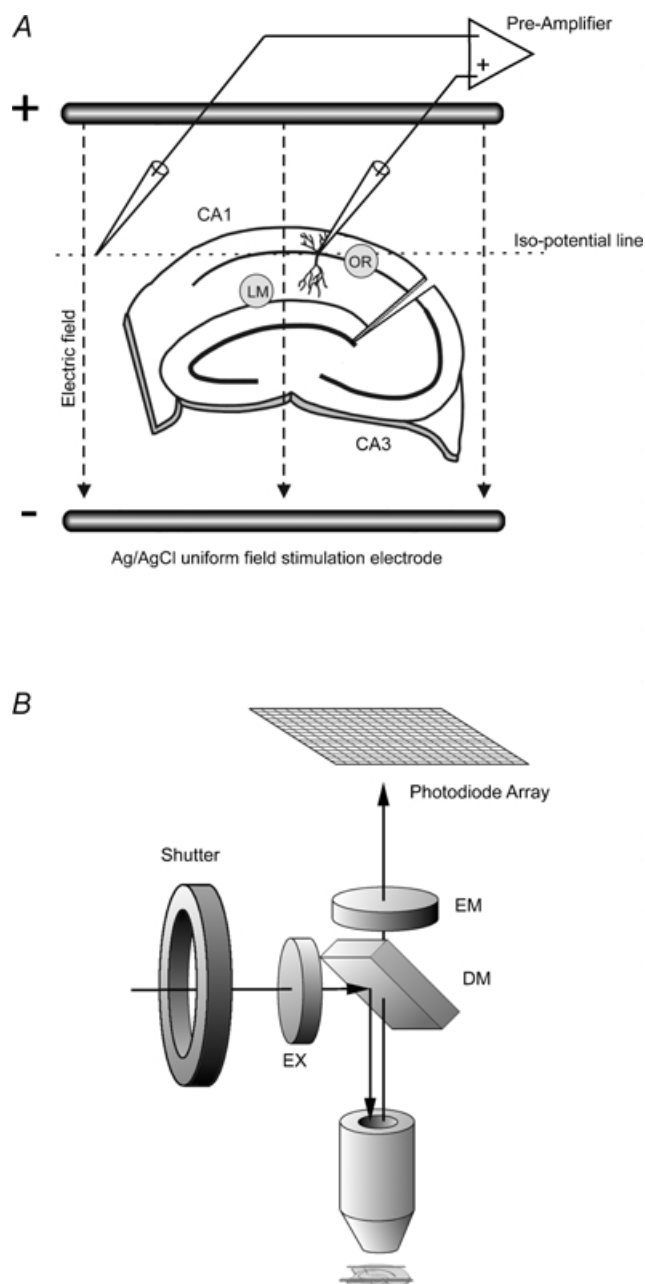


Figure 1. Schematic of electrophysiology and optical mapping experimental design

In all studies, uniform electric fields were generated by passing current between two large parallel silver–silver chloride wires positioned in the bath across the slice. *A*, for electrophysiological measurements activity was monitored in the CA1 pyramidal cell layer with a glass microelectrode. In some experiments, an additional field electrode was positioned in an iso-potential (see text) to remove the uniform field artefact. In some experiments, activity was evoked with a bipolar nichrome stimulating electrode positioned in either stratum lacunosum moleculare (LM) or stratum oriens (OR). (Not to scale.) *B*, schematic drawing of the optical apparatus for fluorescence measurement and the rat hippocampal slice preparation. The microscope objective forms a real magnified image of the preparation at the microscope image

Methods

Electrophysiological studies

Transverse hippocampal slices ($400\ \mu\text{m}$) were prepared from male Sprague-Dawley rats (180–225 g; anaesthetized with intraperitoneal ketamine ($7.4\ \text{mg kg}^{-1}$) and medetomidine ($0.7\ \text{mg kg}^{-1}$) and killed by cervical dislocation). The slices were stored in a holding chamber submerged in artificial cerebrospinal fluid (ACSF) consisting of (mM): 125 NaCl, 26 NaHCO_3 , 3 KCl, 2 CaCl_2 , 1.0 MgCl_2 , 1.25 NaH_2PO_4 , and 10 glucose, bubbled with a mixture of 95% O_2 –5% CO_2 . After $>60\ \text{min}$, slices were transferred to an interface recording chamber at 33°C .

Uniform DC electric fields were generated across individual slices by passing current between two parallel electrodes placed on the surface of the ACSF in the interface chamber (Fig. 1); the wires were parallel to the direction of perfusate flow. Fields were applied using either chlorided Ag wires $>40\ \text{mm}$ long and placed $>15\ \text{mm}$ apart or sintered Ag–AgCl cylindrical pellet electrodes $12\ \text{mm}$ long and placed $>5\ \text{mm}$ apart (which were used for stronger fields). The square waveforms were $<2\ \text{s}$ in duration, unless otherwise stated; they were generated by a Power 1401 signal acquisition system (Cambridge Electronic Design, Cambridge, UK) and converted to a constant current by a stimulus isolation unit (either BSI-1, Bak Electronics, Germantown, MD, USA or 2200, A-M Systems, Carlsborg, WA, USA). The electric field (mV mm^{-1}) in the chamber was measured by two recording electrodes separated by $0.5\ \text{mm}$ and calibrated to the current passed through the Ag–AgCl electrodes (Ghai *et al.* 2000; Durand & Bikson, 2001).

Measurements of the spatial profiles of the electric fields induced in slices and in the adjacent ACSF revealed that the electric field was not affected by the presence of the slice, consistent with previous studies (Andreasen & Nedergaard, 1996; Gluckman *et al.* 1996; Ghai *et al.* 2000; Bikson *et al.* 2001; Deans *et al.* 2003); the presence of a ‘shunting’ fluid around the slice presumably minimizes the effect of the slice inhomogeneity on

plane. A 16×16 array of photodetectors, positioned at the image plane, records the changes in light intensities that are related to neuronal activity. Epi-illumination with a $20\times$, $0.5\ \text{NA}$, long working distance, objective was used. The preparation was illuminated with the green portion (EX: excitation filter $520 \pm 45\ \text{nm}$) of the output of a halogen lamp. Fluorescence emission from the preparation was selected by means of a dichroic mirror (DM: $570\ \text{nm}$) and an emission filter (EM: $590\ \text{nm}$). The output of each detector was individually amplified, multiplexed, digitized and stored in a PC.

the induced field. In experiments in which population activity (e.g. population spikes) was induced, endogenous non-uniform fields would be superimposed. It should be emphasized that endogenous fields were not present in intracellular field sensitivity and optical mapping experiments. The term 'uniform' is consistently used in the literature to distinguish *exogenous* fields applied via large parallel wires, as used here, from 'local' or 'radial' fields applied through a monopolar source, where interpretation is complicated by variations in spatial relationship of the polarizing electrodes, neuronal morphology and the recording site (Durand & Bikson, 2001; Lian *et al.* 2003).

A complete mechanical lesion was made across the CA2 region to cut the CA3 Schaffer collateral input to CA1. Unless otherwise stated, the somato-dendritic axis of the CA1 region was aligned parallel to the direction of the induced field (0 deg); anodal and cathodal polarization on the alveus side of the CA1 region were defined as positive and negative field, respectively (Fig. 1). In some experiments, slices were aligned with the somato-dendritic axis of the CA1 region perpendicular to the direction of the induced field (90 deg); anodal and cathodal polarization on fimbrial end of the hippocampus were defined as positive and negative field, respectively (Fig. 8).

Orthodromic ('synaptic') responses were evoked by brief (200 μ s) stimulation of either the border between stratum oriens and stratum pyramidale, normally in CA1c ('oriens stimulation'), or stratum lacunosum moleculare, normally in CA1a ('LM stimulation'), using a bipolar, nichrome wire (0.05 mm diameter) stimulating electrode (Fig. 1). In the case of oriens stimulation we adjusted the stimulus position and strength to minimize the antidromic population spike (which could be evoked if current spread to the alveus). Orthodromic stimuli were applied at 1.0–0.016 Hz; population spike amplitudes were allowed to stabilize before applying the fields. Control responses were obtained before and after application of polarizing current. Orthodromic stimuli were applied >0.5 s after field application or termination. Unless otherwise stated, orthodromic stimulation intensity was adjusted to produce 30–70% of the maximal control response.

Conventional recording techniques were used to measure activity from the CA1 pyramidal cell region. Extracellular field potentials were recorded with glass micropipettes (2–8 M Ω) filled with normal ACSF. In certain experiments, a second electrode was placed in the bath on an 'isopotential line' (Fig. 1) to allow for differential recording so that neuronal activity could be observed even during significant potential changes induced in the electrolyte by current application

(the 'exogenous potential'). Intracellular electrodes (70–120 M Ω) were filled with 2 M potassium methylsulphate. For intracellular experiments, the voltage recorded by a field electrode (placed within 50 μ m of the impaled neuron) was subtracted from the intracellular potential to obtain the transmembrane voltage and remove the exogenous potential. Signals were: subtracted, amplified, and low-pass filtered (1–10 kHz) with an Axoclamp-1B (Axon Instruments, Union City, CA, USA) and Neurolog NL-106 and NL-125 amplifiers (Digitimer, Hertfordshire, UK); digitized using a Power 1401 and Signal software (Cambridge Electronic Design Ltd, Cambridge, UK); and analysed off-line using Signal (Cambridge Electronic Design Ltd) and MiniAnalysis (Synaptosoft Inc, Decatur, GA, USA).

Population spike amplitude was measured as peak-to-peak of the evoked responses. Population EPSP amplitude was measured as the baseline to peak of the evoked response. The time constant of polarization was calculated as the time to reach 67% of peak transmembrane polarization; any instantaneous polarization was assumed to be due to deviation of the field reference from isopotential (exogenous potential); the amplitude of the exogenous potential was confirmed after each recording with the intracellular electrode outside the cell. One dimensional current source density (CSD) analysis was determined using the equation $CSD = V_{x-1} - 2V_x + V_{x+1}$, where x is the index of electrodes aligned along the apical dendritic axis (Jefferys, 1979). In CSD experiments, AC coupling was used to remove the exogenous potential. Unless otherwise stated, all results are reported as means \pm s.d.; n = number of slices (for extracellular recording and imaging) or cells (for intracellular recording).

Optical imaging

For optical recordings, an upright microscope (BX50WI, Olympus, Tokyo, Japan) was rigidly mounted on a vibration-isolation table (Newport Research, CA, USA). Slices were viewed with a long working distance 20 \times water immersion objective (Olympus UPlanFI 20 \times , 0.50 NA). The system included: a 24 V/300 W halogen lamp, an incident light filter, 480–550 nm, a dichroic mirror with a centre wavelength of 570 nm, and a barrier filter of 590 nm (U-MSWG, Olympus, Tokyo, Japan). Transmitted light was detected by a 16 \times 16 square array of photodiodes (Argus-20/PDA, Hamamatsu Photonics, Hamamatsu, Japan). Each photodiode received light from a 22.5 μ m \times 22.5 μ m area of the objective field. Photocurrents generated at photodiodes were converted to

voltages using current-to-voltage converters with 100 M Ω feedback resistors. They were sampled-and-held and DC-coupled to analog-to-digital converters with a 16-bit resolution. We used a frame rate of 1–2 kHz.

Hippocampal slices (400 μ m) were prepared from male Wistar rats (5–7 weeks old; anaesthetized with ether). Slices whose dendrites were parallel to the surface were chosen by visually identifying the dendrites with infrared differential interference contrast videomicroscopy. Slices were stained in a separate compartment of the storage chamber, containing 130 μ M RH414 (Molecular Probes, Eugene, OR, USA), bubbled with a mixture of 95% O₂–5% CO₂. Slices were stained for 40 min, washed briefly in the storage chamber, and then transferred to a recording chamber. Recordings were made in a superfusion chamber at a temperature of $27.0 \pm 1.0^\circ\text{C}$. A complete mechanical lesion was made across the CA2 region. A pair of Ag–AgCl electrodes was placed on the neocortex and the dentate gyrus to apply uniform electric fields within CA1, parallel to the apical–dendritic axis of its pyramidal neuron (0 deg). The waveforms (400 ms pulses) applied to the wires were generated by a stimulator (Nihon Kodens, Tokyo) and converted to a constant current by a custom-made stimulus isolation unit. Direct transmembrane voltage responses to the applied electric field were optically recorded.

To improve the signal to noise ratio, 64 traces were averaged for each photodiode recording, with further spatial averaging of the data from arrays of 2×8 photodiodes. Dye bleaching was corrected off-line by subtracting the control trace without applying electric fields. Light intensities were measured as relative fluorescence change ($\Delta F/F$), where F is the fluorescent light intensity of the stained slice during illumination without stimulation and ΔF is the fluorescence change during field application. A decrease in fluorescence (plotted upwards in a figure) corresponds to membrane depolarization, and an increase in fluorescence corresponds to membrane hyperpolarization. Time constants of initial responses to applied fields were also determined by a single exponential curve fitting to the optical signals 0–20 ms from the onset of the applied field using Origin 6.1 software (Origin Lab Corp., Northampton, MA, USA).

Results

Effects of electric fields parallel to the soma–dendritic axis on oriens-evoked population spikes

Negative applied uniform fields of up to -80 mV mm^{-1} (cathode on alveus side of CA1) decreased the delay

and increased the amplitude of population spikes evoked by oriens stimulation (38 of 39 slices tested); positive fields increased the delay and decreased the amplitude of population spikes evoked by oriens stimulation (33 of 39 slices; Fig. 2A). Increasing the strength of the applied electric fields enhanced the modulation of population spike amplitude and delay, in a quasi-linear fashion, with no obvious threshold (Fig. 2B). The average population spike amplitude changes during 60 mV mm^{-1} and -60 mV mm^{-1} fields were to $56 \pm 31\%$ control and $211 \pm 45\%$ control, respectively ($P < 0.001$, paired t tests).

Increasing orthodromic stimulus intensity decreased the modulation of population spike amplitude caused

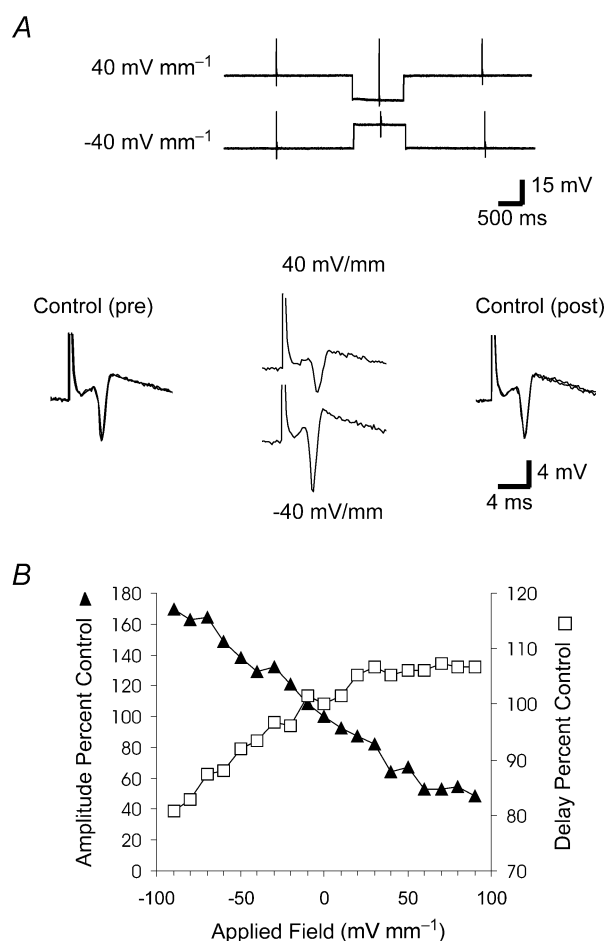


Figure 2. Effect of applied uniform electric fields on population spikes evoked by oriens stimulation

A, top, stimulus protocol. Population spikes were evoked continuously at 0.5 Hz. One-second electric fields were applied 500 ms before the orthodromic pulse. Bottom, population spikes evoked before, during and after application of 40 mV mm^{-1} uniform electric fields. Pre- and post-traces are overlaid. In this and subsequent figures, the orthodromic stimulation artefact is clipped. B, effect of varied amplitude electric fields on population spike amplitude and delay; summary of single slice.

by the applied electric fields. At low (subthreshold) orthodromic stimulus intensities, negative fields dramatically increased population spike amplitude (Fig. 3, top row). As orthodromic stimulus intensity increased, the *relative* increase in population spike amplitude caused by application of negative fields decreased. In response to supra-maximal orthodromic pulses (Fig. 3, bottom), negative fields had no effect on the size of the first evoked population spike. However, at strong stimulus intensities, negative fields could result in the generation of a second population spike. The attenuation of population spike amplitude caused by application of positive fields also decreased as orthodromic stimulus intensity increased (Fig. 3, right column); positive fields had no effect on population spikes evoked by supra-maximal orthodromic stimulation.

All these effects were reversible 500 ms after the end of the field application (Fig. 2A).

Effects of large applied electric fields inducing epileptiform network activity

Large negative fields ($>80 \text{ mV mm}^{-1}$, 1 s) induced epileptiform activity in 19 of the 24 slices tested

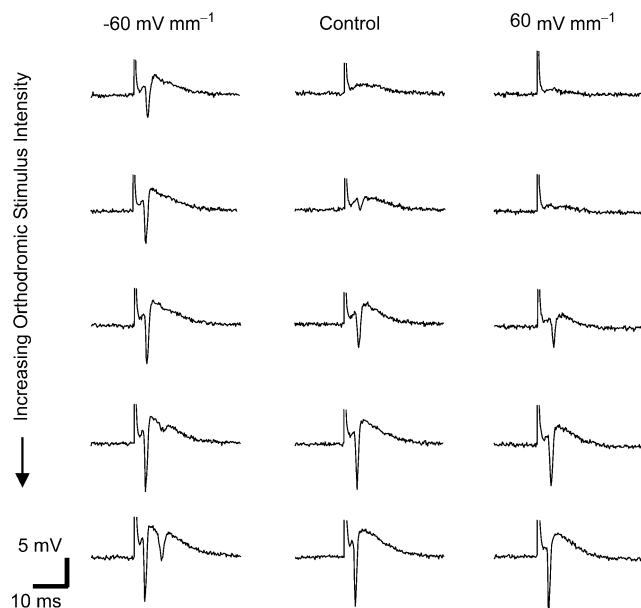


Figure 3. Effect of $\pm 60 \text{ mV mm}^{-1}$ applied electric fields on population spikes evoked by varying intensity orients stimulation

Top to bottom, orthodromic stimulus intensity was incrementally increased. At each orthodromic stimulus intensity, the effect of -60 mV mm^{-1} (middle) and $+60 \text{ mV mm}^{-1}$ (right) electric fields was determined. Note that no spontaneous activity was observed in this slice at these field strengths.

(Fig. 4A, bottom). This epileptiform activity was not blocked (in 5 slices) by the glutamate receptor antagonists D(-)-2-amino-5-phosphonopentanoic acid (D-APV; $50 \mu\text{M}$) and 2,3-dioxo-6-nitro-1,2,3,4-tetrahydrobenzo[f]quinoxaline-7-sulphonamide (NBQX; $20 \mu\text{M}$, added after 20 min), nor by the further addition

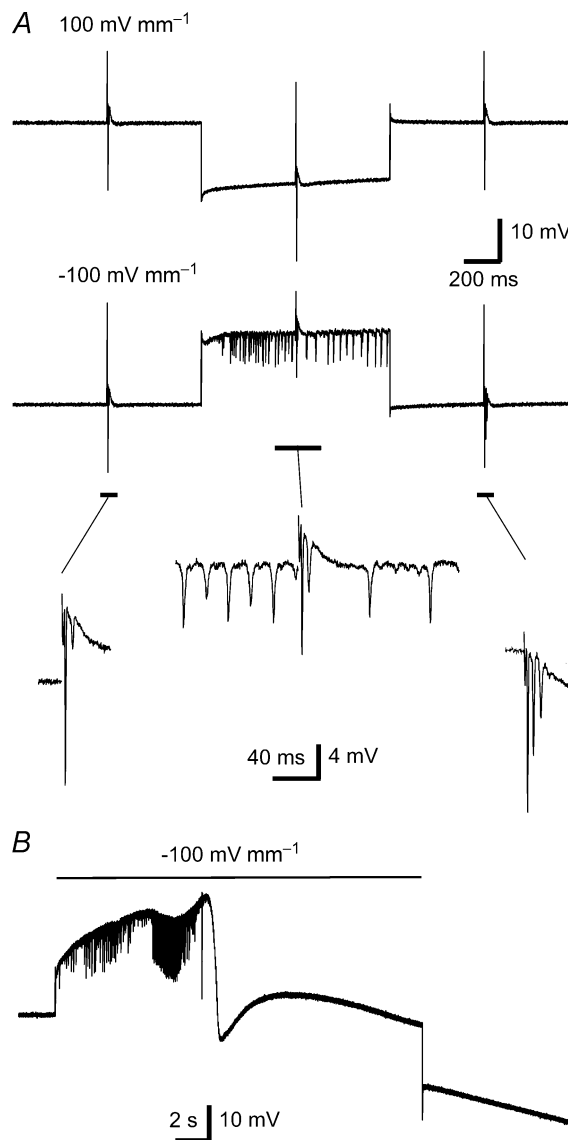


Figure 4. Effect of $\pm 100 \text{ mV mm}^{-1}$ applied electric fields on evoked population spikes and spontaneous activity

A, top, no spontaneous activity was observed in the absence of applied electric fields or after application of $+100 \text{ mV mm}^{-1}$ electric fields. Middle, -100 mV mm^{-1} fields (1.0 second) induced spontaneous epileptiform activity. Population spikes were evoked by orients stimulation continuously at 0.5 Hz. Bottom, expansion of field traces before (left), during (middle), and after (right) application of -100 mV mm^{-1} electric fields. Note that postfield evoked response (right) did not return to control levels (left). The orthodromic stimulus artefact was removed in the expansion insets. B, effect of prolonged application of -100 mV mm^{-1} electric field (bar) on spontaneous activity.

of bicuculline ($25 \mu\text{M}$). Positive fields never induced epileptiform activity, over the full range of strengths tested ($<200 \text{ mV mm}^{-1}$; Fig. 4A, top). During epileptiform bursting induced by negative fields, orthodromically evoked activity showed a decrease in the size of the first population spike and the generation of additional population spikes. If robust epileptiform activity was induced, the modulation of the evoked response could persist for several seconds after the termination of the applied field (Fig. 4A, bottom right).

This epileptiform activity appeared above a threshold field strength; further increases in fields made it more intense. Increasing the applied field from -80 to -100 to -150 mV mm^{-1} (4-s pulses in 3 slices) increased spike frequencies from 14 to 23 to 30 Hz, respectively; maximum population spike amplitudes did not increase with increasing suprathreshold fields. More prolonged ($>5 \text{ s}$) application of large ($>100 \text{ mV mm}^{-1}$) negative fields could trigger an electrographic seizure followed by spreading depression ($n = 3$; Fig. 4B). Episodes of spreading depression were followed by a reduction in orthodromic responses for 2–10 min after termination of the applied field (not shown). A similar long-lasting depression has been shown to follow application of large excitatory steady-state currents *in vivo* (Bindman *et al.* 1964).

Very large positive fields ($>150 \text{ mV mm}^{-1}$) could trigger a single small population spike immediately after field application ('leading-edge excitation'), but not for the remaining duration of field application or after field termination.

Effects of electric fields on LM-evoked population spikes

In contrast to the opposite effects of positive and negative fields on oriens-evoked population spikes, both positive (36 of 50 slices tested) and negative (49 of 50 slices) applied fields increased the amplitude and decreased the delay of population spikes evoked by LM stimulation (Fig. 5A). Increasing the amplitude of the applied fields enhanced the modulation of population spike amplitude and delay (Fig. 5B). The average population spike amplitude changes during 60 mV mm^{-1} and -60 mV mm^{-1} fields were to $122 \pm 46\%$ control and $185 \pm 63\%$ control, respectively ($P < 0.01$ and < 0.001). Taken together with oriens stimulation results, these data suggest that variations in the location of activated synapses along the dendritic axis will contribute to the substantial variation of modulation efficacy across slices. As with oriens stimulation, large negative fields, but never positive fields, could result in

the generation of a second population spike (even in the absence of epileptiform activity).

Multiple channel recording ($n = 8$; Fig. 6) confirmed that LM stimulation can initiate population spikes in the apical dendrites (Turner *et al.* 1991; Golding & Spruston, 1998; Kasuga *et al.* 2003). This was evident from the negative apical dendritic potentials (at $+50$ to $+150 \mu\text{m}$ in Fig. 6C) preceding the population spike in the pyramidal layer (0 to $+50 \mu\text{m}$; bold trace). Furthermore, the current sinks (dark blue) in the contour plot of the current source density measurements showed the first population spike

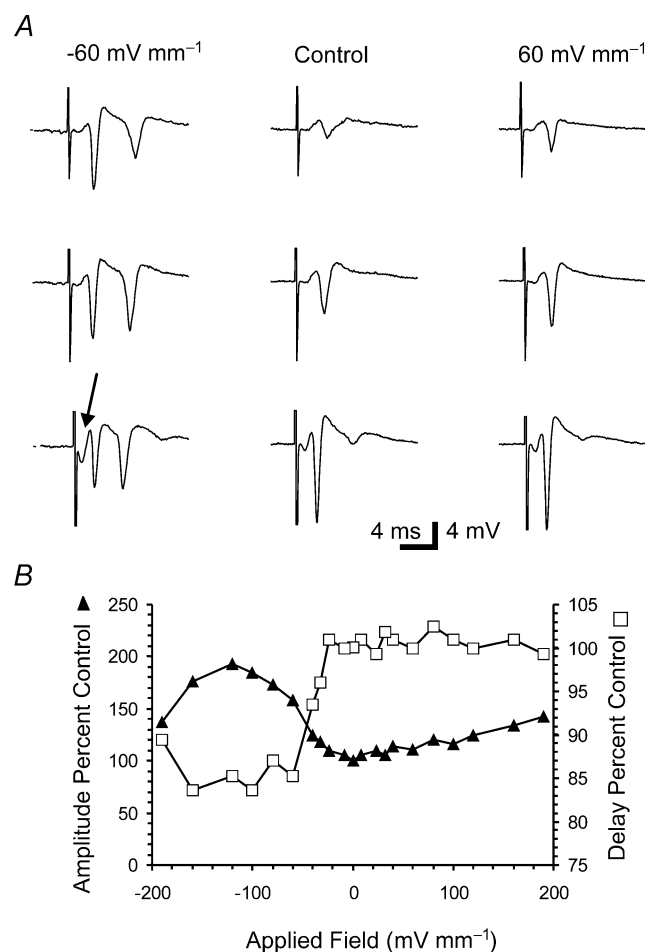


Figure 5. Effect of applied electric fields on population spikes evoked by varying intensity LM stimulation

Population spikes were evoked continuously at 0.5 Hz. One-second electric fields were applied 500 ms before the orthodromic pulse. A, effects of $\pm 60 \text{ mV mm}^{-1}$ fields on population spikes evoked by varied intensity LM orthodromic stimulation. Top to bottom, orthodromic stimulus intensity was incrementally increased. The arrow indicates a presumed 'non-synaptic' spike (see text). B, effect of applied electric fields on first orthodromic evoked population spike amplitude (▲) and delay to this population spike peak (□); summary of single slice. Note that the amplitude of only the orthodromic population spike is plotted (see Results).

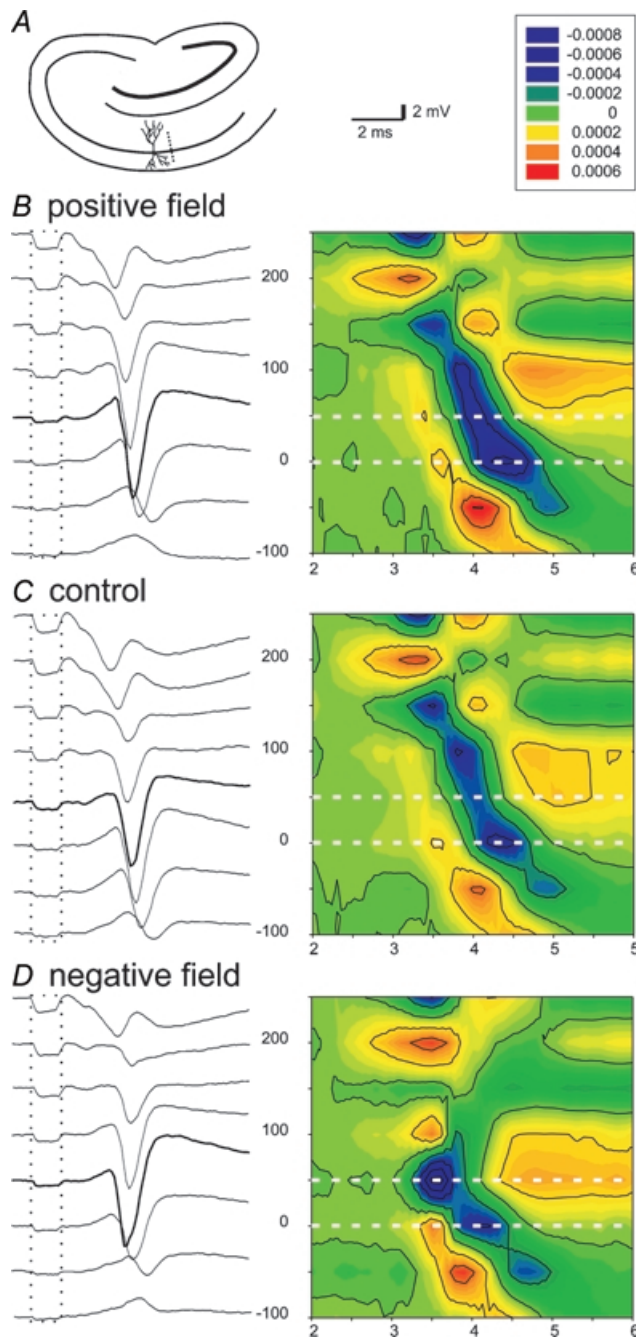


Figure 6. Effect of applied electric fields on population spike initiation zone and population EPSP in response to orthodromic LM stimulation

A, left, supra-threshold activity, evoked by stimulation of stratum lacunosum moleculare, was recorded at a series of sites separated by $50\ \mu\text{m}$ on a line perpendicular to the pyramidal layer (marked by dashed line). B–D, evoked potentials recorded from these sites (left; calibration in A, centre), spatially aligned with a contour plot (right) of the current source densities estimated by the second spatial differences of these potentials (calibration key in mV mm^{-2} is in A, right; sinks are dark blue, sources are yellow; x-axis is time in ms after the stimulus; y-axis is distance in μm from the border between strata oriens and pyramidal). The location of the pyramidal layer is marked by white dashed lines; on this scale the synaptic sink is just visible at

sink at $+100$ to $+150\ \mu\text{m}$ (in stratum radiatum, about $100\ \mu\text{m}$ from the edge of the synaptic sink just visible at the top of the contour plots); the population spike sink then propagated towards the pyramidal layer. Negative applied fields potentiated the population spike recorded at the cell body layer (Fig. 6D, see also Fig. 5 and compare Fig. 2). These negative fields moved the site of population spike initiation from stratum radiatum to stratum pyramidal (evident in both the voltage traces and the current source density contour plot; Fig. 6D); the mean distance of the shift in spike initiation site was $125\ \mu\text{m}$ (5 slices). In contrast, under positive fields LM stimulation continued to initiate population spikes in stratum radiatum, which then propagated to the pyramidal layer (Fig. 6B).

With both oriens and LM orthodromic stimulation strong enough to evoke two population spikes (Fig. 5A, bottom), negative fields potentiated the second population spike and positive fields attenuated the second population spike (independent of the field's effects on the first population spike). This finding is consistent with the second spike always being generated near the soma.

Lastly, negative fields could decrease *orthodromic* population spike amplitude, in the absence of epileptiform activity, in response to high intensity LM or oriens orthodromic stimulation. In these cases, application of negative fields caused the appearance of an additional population spike, preceding the orthodromic population spike (Fig. 5A, arrow). Because of its short delay, this population spike presumably reflects direct 'non-synaptic' activation of neurons. Those neurons activated non-synaptically would be refractory during the orthodromic evoked EPSP, reducing the amplitude of the orthodromic population spike (Fig. 5B left).

Intracellular recording

Intracellular recordings were obtained from a total of 18 pyramidal cells during application of uniform electric fields parallel to the soma–dendritic axis (0°). In all neurons studied, application of exogenous fields generated changes in transmembrane potential (Fig. 7).

the top of the contour plot. C, responses in the absence of applied fields, showing spike initiation in stratum radiatum and propagating to stratum pyramidal (bold trace). B, responses under $+50\ \text{mV mm}^{-1}$ applied DC fields, have a similar pattern to those in C, but are potentiated (see also Fig. 5). D, responses under $-50\ \text{mV mm}^{-1}$ applied fields also are potentiated at the pyramidal layer (bold trace), but in this case the population spike initiation site moved into stratum pyramidal.

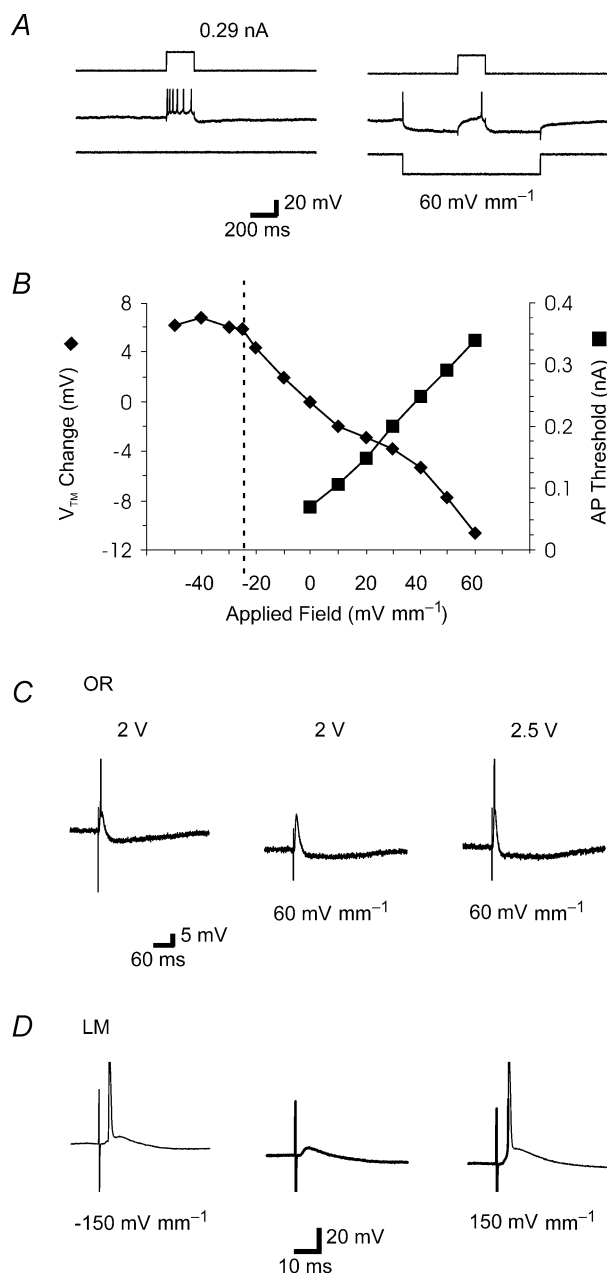


Figure 7. Effect of applied electric fields on single CA1 pyramidal neurons monitored with intracellular sharp microelectrodes

A, left, in the absence of an electric field, intracellular injection of current pulse (200 ms, 0.29 nA) triggered a train of action potentials. In this and the other traces, action potentials are clipped. A, right, application of $+60 \text{ mV mm}^{-1}$ electric fields induced hyperpolarization. Injection of a current pulse (200 ms, 0.29 nA) during field application triggered only a single action potential. B, effect of applied fields on transmembrane potentials (◆) and threshold for triggering a single action potential with an intracellular current pulse (200 ms) during field application (■); summary of single slice. Vertical dashed line indicates the threshold for generation of spontaneous action potential by uniform field application; average transmembrane potential was measured during the interspike interval. C, left, an action potential was evoked by orthodromic stimulation (2 V) in stratum oriens. Middle,

Positive fields resulted in somatic hyperpolarization while negative fields resulted in somatic depolarization. The average time constants for exogenous field induced membrane hyperpolarization ($16 \pm 8 \text{ ms}$ for 60 mV mm^{-1} and $21 \pm 14 \text{ ms}$ for 40 mV mm^{-1}) were not significantly different from the time constants for membrane polarization induced by direct intracellular current injection ($15 \pm 5 \text{ ms}$ and $23 \pm 13 \text{ ms}$ for currents producing similar steady-state hyperpolarization). For fields between -40 and $+60 \text{ mV mm}^{-1}$, the steady-state polarization varied linearly with the strength of the applied electric field with an average sensitivity of $0.12 \pm 0.05 \text{ mV per mV mm}^{-1}$ applied field ($P < 0.001$). Large negative fields induced action potentials, while large positive fields led to activation of 'sag' currents similar to those observed during intracellular current injection. As with direct intracellular current injection, neuronal firing induced by negative fields showed spike frequency adaptation. Negative fields also increased the variance of the membrane potential between action potentials (not shown), presumably reflecting an increase in PSPs concomitant with a general increase in excitability of the large neuronal population.

Positive extracellular applied fields increased the threshold intracellular current needed for action potential generation (Fig. 7A and B). Negative fields decreased action potential threshold, and could polarize the neurons enough to elicit action potentials directly.

The effect of applied fields on action potential threshold in response to oriens stimulation was investigated in three cells. Negative fields decreased action potential threshold. Positive fields suppressed action potential generation in response to just supra-threshold stimuli but not in response to larger orthodromic stimuli (Fig. 7C).

The effect of applied fields on action potential threshold in response to LM stimulation was investigated in eight cells. In four cells, both positive and negative fields decreased action potential threshold (Fig. 7D); in two cells, positive fields decreased action potential threshold and negative fields had no effect on threshold; in the remaining two cells positive fields increased threshold and negative

during application of $+60 \text{ mV mm}^{-1}$ electric fields the same intensity orthodromic stimulus resulted in an EPSP but failed to trigger an action potential. Right, stronger orthodromic stimulation (2.5 V) triggered an action potential during application of a $+60 \text{ mV mm}^{-1}$ electric field. D, orthodromic stimulation intensity was fixed at a level that failed to trigger an action potential in the absence of an applied field (left), but during application of both -150 mV mm^{-1} (middle) and 150 mV mm^{-1} (right) the same stimulus triggered an action potential.

fields decreased threshold (in a manner similar to oriens stimulation). The likelihood of fields affecting action potential generation increased with the field strength. When positive fields reduced action potential threshold they also increased subthreshold EPSP amplitude (to $133 \pm 18\%$ for $+50 \text{ mV mm}^{-1}$ fields; $P < 0.04$); negative fields had variable and inconsistent effects on EPSPs (to $174 \pm 140\%$, with -50 mV mm^{-1} fields; $P = 0.37$).

Synaptic field potentials

In 7 of 9 slices, we found that positive fields (hyperpolarizing in the soma and depolarizing in the dendrites) increased population EPSP amplitude, evoked by LM stimulation, and measured extracellularly in stratum radiatum (average change to $127 \pm 34\%$ control for $+60 \text{ mV mm}^{-1}$ field; $n = 9$; $P = 0.05$; Fig. 8). In 8 of 9 slices, negative fields decreased population EPSP amplitude (average change to $70 \pm 34\%$ control for -60 mV mm^{-1} field; $P = 0.04$; $n = 9$). To test whether depolarization of the apical dendrites by positive electric fields enhanced population spike and population EPSP amplitude during LM stimulation by unblocking NMDA channels (Otmakhova *et al.* 2002), we added the NMDA-receptor antagonist D-APV ($25\text{--}50 \mu\text{M}$). The increases in population EPSP and population spike amplitude by positive fields were still observed in the presence of D-APV ($n = 3$, Fig. 8). The decreases in EPSP with negative fields cannot explain the associated potentiation of orthodromic population spikes. With positive fields, increases in EPSP would contribute to the potentiation of orthodromic population spikes, although this was not always the case: the example in Fig. 6 showed virtually no change in the rate of rise of the EPSP (to 101%) with positive fields, despite the potentiation of the population spike to 140% .

Effects of fields applied perpendicular to the somato-dendritic axis

Orthodromic population spikes were modulated by fields applied perpendicular to the somato-dendritic axis (90° deg, Fig. 9A). In all nine slices tested with oriens stimulation on the fimbrial side of the recording site, fimbria-positive fields decreased population spike amplitude (average change to $31 \pm 26\%$ control during 60 mV mm^{-1} field; $n = 4$; $P = 0.013$), while negative fields increased population spike amplitude (average change to $233 \pm 79\%$ control during -60 mV mm^{-1} ; $n = 4$; $P = 0.044$; Figs 9C and D). In all 16 slices tested with LM stimulation on the subicular side of the recording site (as normally used in this

study) fimbria-positive fields increased population spike amplitude (average change to $175 \pm 37\%$ control during 60 mV mm^{-1} ; $n = 11$; $P < 0.001$) while fimbria-negative fields decreased population spike amplitude (average change to $40 \pm 23\%$ control during -60 mV mm^{-1} ; $n = 11$; $P < 0.001$; Fig. 9E). By contrast, when LM stimulation was applied to the fimbrial side of the recording site the changes reversed so that fimbria-positive fields decreased population spike amplitude (average change to $35 \pm 23\%$ control during 60 mV mm^{-1} , $n = 4$; $P = 0.01$), while negative fields increased population spike amplitude (average change to $181 \pm 49\%$ control during -60 mV mm^{-1} ; $P = 0.046$).

The relative enhancement of population spike amplitude (in both oriens and LM stimulation) decreased at fields $>|150| \text{ mV mm}^{-1}$; however, no spontaneous epileptiform activity ($>400 \mu\text{V}$) or 'non-synaptic' activation (see above) was observed at any field strengths tested (Fig. 9C). At the onset of large ($>100 \text{ mV mm}^{-1}$) positive or negative fields, population spikes were evoked (Fig. 9C1). The threshold for 'leading edge excitation' was lower for positive fields (see below).

A total of eight pyramidal cells were recorded intracellularly during application of fields at 90° deg. In contrast with the results for fields at 0° deg, fields of $\pm 60 \text{ mV mm}^{-1}$ had no consistent effect on membrane polarization (average steady-state sensitivity $-0.008 \pm 0.015 \text{ mV per mV mm}^{-1}$ applied field; Fig. 9B; not significantly different from zero). This is striking given that the sensitivity of evoked population spikes to fields applied at 90° deg was very close to that at 0° deg. Both positive and negative fields at 90° deg increased the frequency of events resembling PSPs in 5 of 8 neurons (Fig. 9B); mean frequency increased from 2 s^{-1} to 7.1 s^{-1} for 100 mV mm^{-1} fields ($P < 0.02$) and from 2.7 s^{-1} to 10.5 s^{-1} for 150 mV mm^{-1} fields ($P < 0.0001$). Together these observations suggest that 90° deg polarization modulates the excitability of afferents

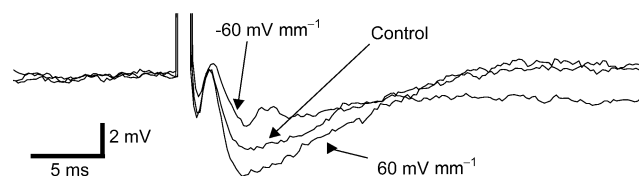


Figure 8. Effects of applied electric fields on population EPSPs Sub-threshold responses (population EPSP), evoked by LM stimulation, were recorded with a single electrode in stratum radiatum in the presence of D-APV, in the absence of applied current ('control'), and during application of $+60 \text{ mV mm}^{-1}$ or -60 mV mm^{-1} electric fields (as labelled).

rather than the postsynaptic pyramidal cells. The lack of antidromic action potentials under 90 deg polarization indicates that the pyramidal cell axons were not polarized sufficiently to reach threshold.

Both large positive and large negative fields could evoke single action potentials at field initiation (Fig. 9B). The threshold for triggering an action potential was lower for fimbria-positive fields than for negative fields

(7 of 8 cells). Action potentials were never observed during the remaining duration of field application or when fields were turned off (i.e. after the trailing edge). Two lines of evidence suggest that 'leading-edge' population spikes/action potentials could be both synaptic (orthodromic) and non-synaptic in nature: action potentials/population spikes could be initiated immediately after field application (non-synaptic) and/or

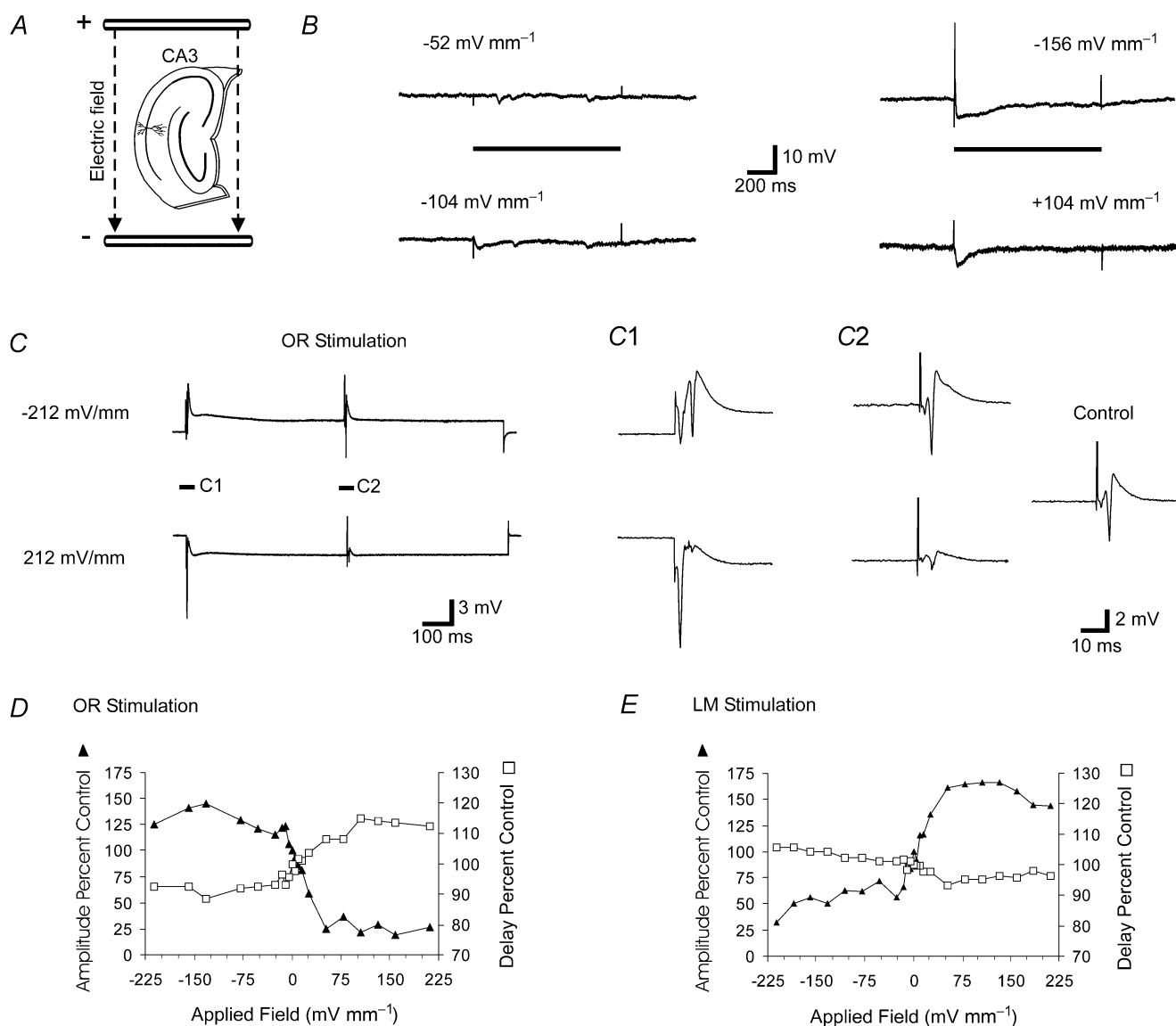


Figure 9. Effect of electric fields applied perpendicular to the soma-dendritic axis

A, schematic diagram illustrating slice orientation at +90 deg and field sign convention. B, intracellular recording of transmembrane potential from a CA1 pyramidal cell during application of fields (bar). C, field recording from CA1 pyramidal cell layer during application of fields. A population spike was evoked by oriens stimulation 500 ms after field application. C1, expansion of field onset in trace C. C2, expansion of orthodromic population spikes during field application in trace C and orthodromic population spike in absence of fields (control). Note the orthodromic and non-synaptic 'leading edge excitation' at field onset (see Results), while field termination is associated with a capacitive artefact but no population spikes. D and E, summary of effect of electric fields applied at 90 deg on population spike amplitude and delay in response to CA1a oriens (D) and CA1c LM (E) stimulation.

after a brief delay, superimposed on intracellular and 'population' EPSPs (orthodromic). 'Orthodromic' but not 'non-synaptic' population spikes could be suppressed after addition of the AMPA receptor antagonist CNQX ($n = 2$, not shown). Large positive or negative fields could also trigger an apparent IPSP at their onset, presumably due to the direct activation of interneurons.

Imaging with voltage sensitive dyes

Transmembrane voltage changes in response to applied uniform electric fields were measured using optical recording ($n = 6$). Application of positive electric fields (40 mV mm^{-1}), at 0 deg, induced a monophasic hyperpolarization, with a relatively slow time constant, in the CA1 pyramidal layer, and a biphasic response in the apical dendrites consisting of a relatively rapid depolarization followed by a slow (partial) repolarization (Fig. 10B). Application of negative electric fields (-40 mV mm^{-1}) induced similar changes with opposite polarities. The time constants of initial polarization (0–20 ms from the onset of applied field) of transmembrane potentials varied across the somato-dendritic axis (Table 1). Faster time constants were observed in dendritic regions than in the somatic layer. Spatial profiles of the distribution of transmembrane voltage responses are shown in Fig. 10C. The reversal of the transmembrane potential (the 'zero-polarization point') occurred at a mean of $165 \mu\text{m}$ from the pyramidal layer (20 ms after field onset), rather more proximal than a previous estimate of $300 \mu\text{m}$ based on intradendritic recordings (Andreasen & Nedergaard, 1996), which could be affected by penetration-induced shunts (Svirskis *et al.* 1997). In all six cases contributing to Fig. 10, the 'zero-polarization point' shifted towards the distal apical dendrites during the course of the field application; interpolation revealed this was by $31.6 \pm 3.7 \mu\text{m}$ for positive (basal to apical) fields, and by $29.2 \pm 4.8 \mu\text{m}$ with negative fields. The magnitudes of the optical responses to the -40 mV mm^{-1} electric field were below 0.05%; far smaller than the subthreshold population EPSP (about 0.2%) or population spikes (about 0.6%) of CA1 pyramidal neurons (Inoue *et al.* 2001).

Optical responses were not detected when electric fields (40 mV mm^{-1}) were applied perpendicular (90 deg) to the apical-dendritic axis of the pyramidal neuron (data not shown), suggesting the optical responses were derived mainly from CA1 neurons and not from the membranes of other elements such as glial cells, interneurons or axons. Note that an *asynchronous* increase in membrane noise would not be detected by the optical technique. The faster somatic time constant measured using

intracellular electrodes could result from impalement-induced conductance increase (Spruston & Johnston, 1992).

Discussion

The consensus from previous reports examining the effects of DC fields on neuronal function (Creutzfeldt *et al.* 1962; Purpura & McMurtry, 1965; Jefferys, 1981; Tranchina & Nicholson, 1986; Chan & Nicholson, 1986; Gluckman *et al.* 1996; Durand & Bikson, 2001) was that the modulation of neuronal excitability is a relatively simple function of the orientation of neuronal processes with respect to the applied fields, i.e. positive/negative fields induce somatic hyper-/depolarization which decreases/increases excitability. Our results show that the effects of DC fields are more complex: the polarization of cell membranes has a time constant ($>10 \text{ ms}$) that varies across the cell axis, polarization can be biphasic, fields can induce transient responses at onset, fields can modulate neuronal processing of afferent synaptic input through polarization of dendrites (changing EPSP amplitude or moving of the action potential initiation zone) and through polarization of afferent axons (and thus even at field orientations that do not consistently polarize somata/dendrites), and uniform DC fields, through activation of non-linear processes, can have effects that outlast the duration of the applied fields. The observations contradict hypotheses 2–4 advanced in the Introduction.

Effect of applied fields on CA1 pyramidal cell membrane polarization

The influence of the field on transmembrane potential is related to the second differential of the extracellular potential distribution along the neuron (McNeal, 1976; Tranchina & Nicholson, 1986; McIntyre & Grill, 1999; Rattay, 1999); by definition, a uniform electric field has zero second spatial differential. Thus, a homogeneous non-branching cable of membrane would polarize only (electrotonically) near its ends, depolarizing at the end nearer the cathode and hyperpolarizing at the end nearer the anode. The length constant and the branching geometry of real neurons would determine how localized the polarization is within the dendrites; our finding that pyramidal neurons polarize along the entire neuronal axis is consistent with an electrotonically compact structure (Carnevale *et al.* 1997).

We revealed a novel 'biphasic' polarization in the apical dendrites when fields were applied parallel to the somato-dendritic axis. This was associated with a small shift in

the zero-polarization point. For moderate positive and negative field strengths, the symmetry in polarization profile (Fig. 10, Table 1) indicates that passive, rather than active voltage-dependent, membrane properties are responsible. This could occur if time constants vary along the dendritic tree, for example at branch points which cannot be transformed to an equivalent cylinder (Rall

& Rinzel, 1973), or at local regions of low membrane resistance, as demonstrated in an analysis of penetration injury due to sharp electrodes (Svirskis *et al.* 1997). To our knowledge the present report is the first experimental demonstration in healthy neurons of passive axial currents causing a time-dependent polarization profile (Warman *et al.* 1992).

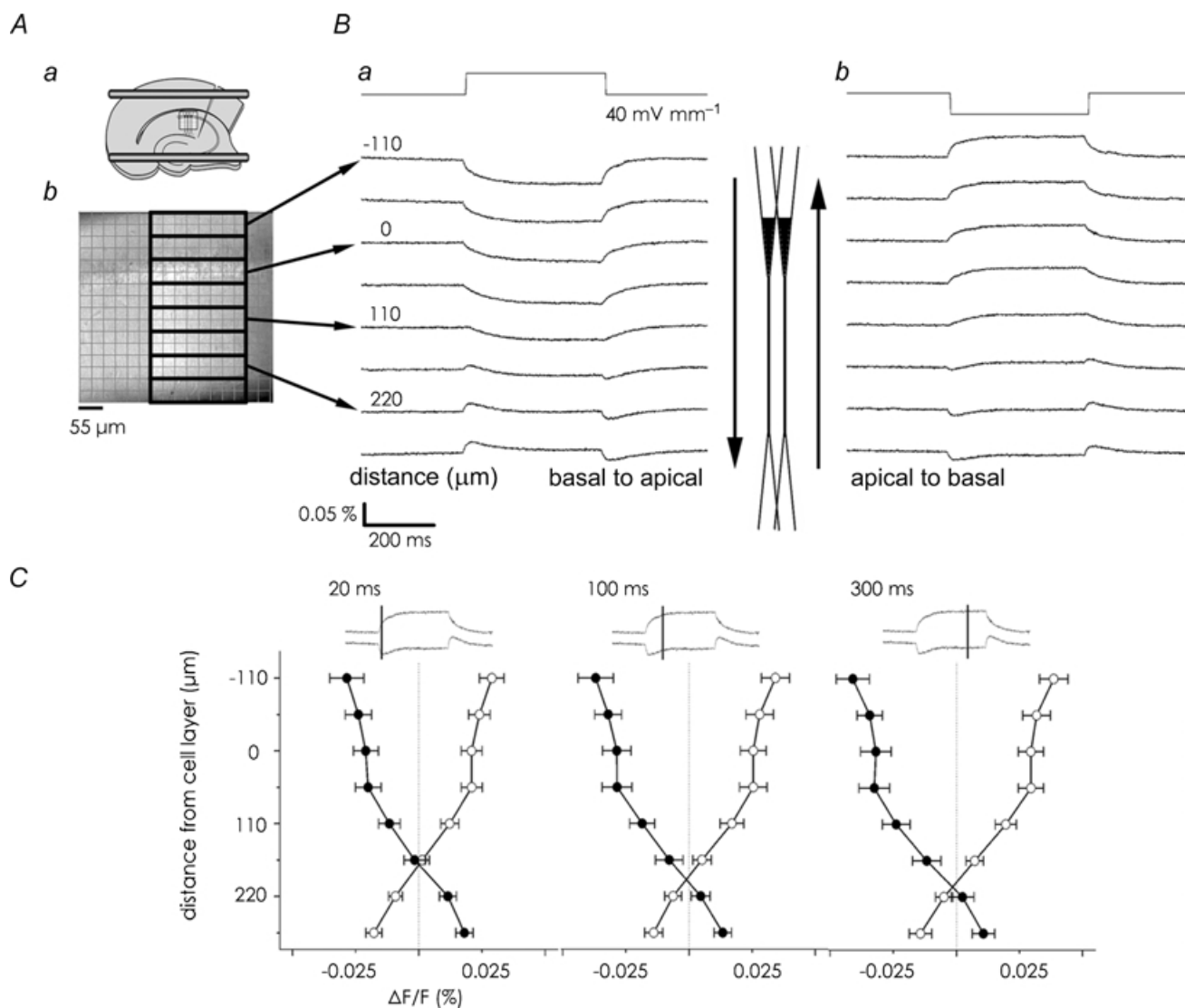


Figure 10. Optical measurement of direct voltage responses to extracellularly applied electrical fields in the CA1 region of the hippocampus

A, hippocampal slice was stained with a voltage sensitive dye RH414. a, parallel field electrodes were placed so as to apply electric fields parallel to the somato-dendritic axis of CA1 pyramidal neurons. Optical responses of CA1 region were monitored using a 20 \times objective lens and a 16 \times 16 square array of photodiodes. b, the CA1 region of the hippocampal slice captured by a CCD camera. Each square corresponds to an objective field of one photodiode. B, optical signals along the somato-dendritic axis of the CA1 pyramidal neurons corresponding to the transmembrane voltage responses to applied electric fields (400 ms duration, 40 mV mm^{-1}) from basal to apical dendrites of CA1 pyramidal neurons (a), and apical to basal dendrites (b). C, distribution of the mean (\pm S.E.M.) magnitudes of the fluorescence change along the somato-dendritic axis of the CA1 pyramidal neurons at 20 (left), 100 (middle) or 300 ms (right) after onset of the electric field ($n = 6$ slices). The electric field was applied from basal to apical dendrites (\bullet) or from apical to basal dendrites (\circ) of the CA1 pyramidal neurons.

Table 1. Time course of polarization across CA1 stratum in response to application of uniform DC fields as detected by optical mapping with voltage sensitive dyes

Region	Distance from soma (μm)	Time constant (ms)		Time to 67% peak (ms)	
		+40 mV mm ⁻¹	-40 mV mm ⁻¹	+40 mV mm ⁻¹	-40 mV mm ⁻¹
Basal dendrite	-110	8.26 \pm 0.69	8.52 \pm 0.73	54.17 \pm 9.08	57.04 \pm 11.76
Soma	0	10.73 \pm 1.87	10.85 \pm 1.39	70.33 \pm 12.19	70.01 \pm 8.89
Apical dendrite	275	8.30 \pm 1.13	7.91 \pm 0.59	14.17 \pm 1.35	13.52 \pm 0.99

Time constants of initial (0–20 ms) optical responses and time to 67% peak (means \pm S.E.M., $n = 6$) in response to application of ± 40 mV mm⁻¹ fields.

As field strengths increase, the polarization profile becomes more complex, because the neuronal polarization can become large enough to affect voltage-sensitive membrane conductances; the concomitant changes in membrane resistance will, in turn, affect the influence of the applied field.

Effect of applied fields on CA1 pyramidal cell function

We propose that the varied, and apparently complex, effects of electric fields on neuronal responses to afferent input can be largely explained on the basis of the polarization effects described above. For oriens stimulation, the spike initiation zone is near the soma, which is depolarized by negative fields and hyperpolarized by positive fields parallel to the somato-dendritic axis. LM stimulation is known to produce EPSPs in the apical dendrite (Inoue *et al.* 2001) which can activate dendritic voltage-gated sodium conductances (Turner *et al.* 1991; Golding & Spruston, 1998; Kasuga *et al.* 2003), a process that will be modulated by changes in dendritic transmembrane potentials resulting from the applied fields. Alveus-negative fields potentiate LM-evoked population spikes by depolarizing the cell bodies, and thus shifting the initiation site to stratum pyramidale. Alveus-positive fields (hyperpolarizing at the soma, depolarizing in the dendrite) also potentiate LM-evoked population spikes; this decrease in threshold could result from several factors. (1) An NMDA-receptor-independent increase in EPSP amplitude, as shown using population EPSP, CSD and intracellular recording, which could be due to axon polarization resulting from the orientation and/or bending of the perforant path fibres. (2) Potentiation of action potential generation at the initiation zone in the apical dendrites. Given that this zone is just proximal to the polarization reversal (Fig. 10), this potentiation may be due to a minority of neurons initiating action potentials at their somata under control conditions, but, under positive fields, shifting the initiation site to the less hyperpolarized

apical dendrites; the resulting increased synchrony would increase population spike amplitude.

Large negative DC fields could induce robust synchronized neuronal firing. We found that large soma-positive fields did not cause these epileptiform discharges, although they are reported to be capable of triggering dendritic spikes (Andreasen & Nedergaard, 1996). The synchronous discharges induced by negative fields were not blocked by D-APV, NBQX, or bicuculline, suggesting that they depend on non-synaptic synchronizing mechanisms, as found in low-calcium field bursts (Jefferys & Haas, 1982). Polarization-induced synchronous discharges represent a novel model of *in vitro* epileptogenesis, because they require neither ionic, nor pharmacological perturbation, nor synchronizing electrical drive; they demonstrate that a tonic increase in excitability is sufficient in itself to trigger electrographic seizure activity.

By inducing repetitive neuronal firing, DC fields could generate long-lasting (>60 s) changes in extracellular ionic activities and extracellular space fraction (Jefferys, 1995). In addition, intense neuronal firing can induce long-term (>60 min) changes in single cell and system function including changes in excitability (Gartside, 1968*b*), synaptic efficacy, and protein expression (Gartside, 1968*a*).

We found that large negative fields could also *decrease* evoked orthodromic population spike amplitude either by inducing spontaneous activity or by decreasing somatic threshold enough to allow focal stimulation to trigger neuronal firing non-synaptically (i.e. without requiring the release of neurotransmitters); both increase the number of neurons in a refractory state during the evoked orthodromic EPSP.

In this report we directly demonstrate, for the first time, that rotation of pyramidal cells dramatically decreases the effect of applied fields on transmembrane potentials in pyramidal cells, but continues to affect synaptically evoked responses (cf. dentate granule cells; Jefferys, 1981).

The continued effect of fields applied perpendicularly to the somato-dendritic axis (90 deg) on pyramidal cell synaptic responses depended on the relative positions of the recording and stimulation sites in the voltage gradient. The simplest explanation for this is that when the stimulus was towards the negative end of the field, the axons in the vicinity would tend to depolarize and become more excitable, resulting in the larger EPSP. Given that axons are long in relation to their space constants, this would depend on the axons terminating (for instance where they were cut during slicing) or bending in relation to the field (Tranchina & Nicholson, 1986; Warman *et al.* 1992; McIntyre & Grill, 1999).

General implications

The present results show that polarization of axons and dendrites, in addition to the cell body (Jefferys, 1981), can affect neuronal responses to afferent input. They also show that effects on afferent fibres should be considered in interpreting the short- and long-term effects of *non-uniform* fields induced by steady-state currents in humans (Nitsche & Paulus, 2001; Liebetanz *et al.* 2002) and other animals *in vivo* (Purpura & McMurtry, 1965; Purpura & Malliani, 1966; Gartside, 1968*b*). Together with the complex and long-term effects of regenerative processes, these factors could also provide an explanation for the (variable) effects of low intensity steady state (Bawin *et al.* 1986; Trabulsi *et al.* 1996), low-frequency AC (Bawin *et al.* 1984; Bawin *et al.* 1986), and radio-frequency (Tattersall *et al.* 2001) electromagnetic fields on orthodromic responses *in vitro*, where these factors were not strictly controlled.

To our knowledge, the present study reports the first direct measurement of membrane time constant (ranging from 14 to 70 ms) for polarization by electric fields. This indicates that neurons will be less sensitive to relatively fast AC electric fields (>15 Hz), whether exogenous or endogenous (Blackwell, 1986; Jefferys, 1995).

Our experimental demonstration that mammalian pyramidal neuron somata polarize linearly with (moderate) field strengths, with a sensitivity of 0.12 mV per mV mm⁻¹ (Fig. 7), is consistent with predictions from computer models (McNeal, 1976; Tranchina & Nicholson, 1986; McIntyre & Grill, 1999; Rattay, 1999) and with observations in turtle cerebellum (Chan *et al.* 1988). This linearity implies that very low-amplitude electric fields could theoretically affect the excitability of neurons close to threshold and that determining an 'absolute' safety limit for electric field exposure may therefore be impractical. Coherent network activity, for example, with

large numbers of neurons oscillating close to threshold may be particularly sensitive to small (below noise levels) synchronized perturbations of pre- and postsynaptic potentials (Valberg *et al.* 1997; Traub *et al.* 1999; Deans *et al.* 2003; Francis *et al.* 2003).

References

- Andreasen M & Nedergaard S (1996). Dendritic electrogenesis in rat hippocampal CA1 pyramidal neurons: functional aspects of Na⁺ and Ca²⁺ currents in apical dendrites. *Hippocampus* **6**, 79–95.
- Bawin SM, Sheppard AR, Mahoney MD, Abu-Assal M & Adey WR (1986). Comparison between the effects of extracellular direct and sinusoidal currents on excitability in hippocampal slices. *Brain Res* **362**, 350–354.
- Bawin SM, Sheppard AR, Mahoney MD & Adey WR (1984). Influences of sinusoidal electric fields on excitability in the rat hippocampal slice. *Brain Res* **323**, 227–237.
- Benabid AL, Koudsie A, Pollak P, Kahane P, Chabardes S, Hirsch E, Marescaux C & Benazzouz A (2000). Future prospects of brain stimulation. *Neurol Res* **22**, 237–246.
- Bikson M, Lian J, Hahn PJ, Stacey WC, Sciortino C & Durand DM (2001). Suppression of epileptiform activity by high frequency sinusoidal fields in rat hippocampal slices. *J Physiol* **531**, 181–191.
- Bindman LJ, Lippold OJC & Redfearn JWT (1964). The action of brief polarizing currents on the cerebral cortex of the rat (1) during current flow and (2) in the production of long-lasting after-effects. *J Physiol* **172**, 369–382.
- Blackwell RP (1986). Effects of extremely-low-frequency electric fields on neuronal activity in rat brain. *Bioelectromagnetics* **7**, 425–434.
- Carnevale NT, Tsai KY, Claiborne BJ & Brown TH (1997). Comparative electrotonic analysis of three classes of rat hippocampal neurons. *J Neurophysiol* **78**, 703–720.
- Chan CY, Hounsgaard J & Nicholson C (1988). Effects of electric fields on transmembrane potential and excitability of turtle cerebellar Purkinje cells *in vitro*. *J Physiol* **402**, 751–771.
- Chan CY & Nicholson C (1986). Modulation by applied electric fields of Purkinje and stellate cell activity in the isolated turtle cerebellum. *J Physiol* **371**, 89–114.
- Creutzfeldt OD, Fromm G & Kapp H (1962). Influences of transcortical D.C. currents on cortical neuronal activity. *Exp Neurol* **5**, 436–452.
- Deans JK, Bikson M, Fox JE & Jefferys JGR (2003). Effects of AC fields at powerline frequencies on gamma oscillations in vitro. Program No. 258.1 2003 Abstract Viewer/Itinerary Planner. Washington DC: Society for Neuroscience On-line.
- Durand DM & Bikson M (2001). Suppression and control of epileptiform activity by electrical stimulation: a review. *Proc IEEE* **89**, 1065–1082.
- Francis JT, Gluckman BJ & Schiff SJ (2003). Sensitivity of neurons to weak electric fields. *J Neurosci* **23**, 7255–7261.

- Freude G, Ullsperger P, Eggert S & Ruppe I (1998). Effects of microwaves emitted by cellular phones on human slow brain potentials. *Bioelectromagnetics* **19**, 384–387.
- Gartside IB (1968a). Mechanisms of sustained increases of firing rate of neurons in the rat cerebral cortex after polarization: role of protein synthesis. *Nature* **220**, 383–384.
- Gartside IB (1968b). Mechanisms of sustained increases of firing rate of neurons in the rat cerebral cortex after polarization: reverberating circuits or modification of synaptic conductance? *Nature* **220**, 382–383.
- Ghai RS, Bikson M & Durand DM (2000). Effects of applied electric fields on low-calcium epileptiform activity in the CA1 region of rat hippocampal slices. *J Neurophysiol* **84**, 274–280.
- Gluckman BJ, Neel EJ, Netoff TI, Ditto WL, Spano ML & Schiff SJ (1996). Electric field suppression of epileptiform activity in hippocampal slices. *J Neurophysiol* **76**, 4202–4205.
- Golding NL & Spruston N (1998). Dendritic sodium spikes are variable triggers of axonal action potentials in hippocampal CA1 pyramidal neurons. *Neuron* **21**, 1189–1200.
- Grill WM & Kirsch RF (2000). Neuroprosthetic applications of electrical stimulation. *Assist Technol* **12**, 6–20.
- Inoue M, Hashimoto Y, Kudo Y & Miyakawa H (2001). Dendritic attenuation of synaptic potentials in the CA1 region of rat hippocampal slices detected with an optical method. *Eur J Neurosci* **13**, 1711–1721.
- Jefferys JGR (1979). Initiation and spread of action potentials in granule cells maintained *in vitro* in slices of guinea-pig hippocampus. *J Physiol* **289**, 375–388.
- Jefferys JGR (1981). Influence of electric fields on the excitability of granule cells in guinea-pig hippocampal slices. *J Physiol* **319**, 143–152.
- Jefferys JGR (1995). Non-synaptic modulation of neuronal activity in the brain: electric currents and extracellular ions. *Physiol Rev* **75**, 689–723.
- Jefferys JGR & Haas HL (1982). Synchronized bursting of CA1 pyramidal cells in the absence of synaptic transmission. *Nature* **300**, 448–450.
- Kasuga A, Enoki R, Hashimoto Y, Akiyama H, Kawamura Y, Inoue M, Kudo Y & Miyakawa H (2003). Optical detection of dendritic spike initiation in hippocampal CA1 pyramidal neurons. *Neuroscience* **118**, 899–907.
- Lian J, Bikson M, Sciortino C, Stacey WC & Durand DM (2003). Local suppression of epileptiform activity by electrical stimulation in rat hippocampus *in vitro*. *J Physiol* **547**, 427–434.
- Liebetanz D, Nitsche MA, Tergau F & Paulus W (2002). Pharmacological approach to the mechanisms of transcranial DC-stimulation-induced after-effects of human motor cortex excitability. *Brain* **125**, 2238–2247.
- McIntyre CC & Grill WM (1999). Excitation of central nervous system neurons by nonuniform electric fields. *Biophys J* **76**, 878–888.
- McNeal DR (1976). Analysis of a model for excitation of myelinated nerve. *IEEE Trans Biomed Eng* **23**, 329–337.
- Nitsche MA & Paulus W (2000). Excitability changes induced in the human motor cortex by weak transcranial direct current stimulation. *J Physiol* **527**, 633–639.
- Nitsche MA & Paulus W (2001). Sustained excitability elevations induced by transcranial DC motor cortex stimulation in humans. *Neurology* **57**, 1899–1901.
- Otmakhova NA, Otmakhov N & Lisman JE (2002). Pathway-specific properties of AMPA and NMDA-mediated transmission in CA1 hippocampal pyramidal cells. *J Neurosci* **22**, 1199–1207.
- Purpura DP & Malliani A (1966). Spike generation and propagation initiated in the dendrites by transhippocampal polarization. *Brain Res* **1**, 403–406.
- Purpura DP & McMurtry JG (1965). Intracellular activities and evoked potential changes during polarization of motor cortex. *J Neurophysiol* **28**, 166–185.
- Rall W & Rinzel J (1973). Branch input resistance and steady attenuation for input to one branch of a dendritic neuron model. *Biophys J* **13**, 648–687.
- Rattay F (1999). The basic mechanism for the electrical stimulation of the nervous system. *Neuroscience* **89**, 335–346.
- Richardson TL, Turner RW & Miller JJ (1984). Extracellular fields influence transmembrane potentials and synchronization of hippocampal neuronal activity. *Brain Res* **294**, 255–262.
- Saunders RD & Jefferys JGR (2002). Weak electric field interactions in the central nervous system. *Health Phys* **83**, 366–375.
- Spruston N & Johnston D (1992). Perforated patch-clamp analysis of the passive membrane properties of three classes of hippocampal neurons. *J Neurophysiol* **67**, 508–529.
- Svirskis G, Gutman A & Hounsgaard J (1997). Detection of a membrane shunt by DC field polarization during intracellular and whole cell recording. *J Neurophysiol* **77**, 579–586.
- Tattersall JE, Scott IR, Wood SJ, Nettell JJ, Bevir MK, Wang Z, Somasiri NP & Chen X (2001). Effects of low intensity radiofrequency electromagnetic fields on electrical activity in rat hippocampal slices. *Brain Res* **904**, 43–53.
- Trabulsi R, Pawlowski B & Wieraszko A (1996). The influence of steady magnetic fields on the mouse hippocampal evoked potentials *in vitro*. *Brain Res* **728**, 135–139.
- Tranchina D & Nicholson C (1986). A model for the polarization of neurons by extrinsically applied electric fields. *Biophys J* **50**, 1139–1156.
- Traub RD, Jefferys JGR & Whittington MA (1999). *Fast Oscillations in Cortical Circuits*. MIT Press, Cambridge, MA, USA.
- Turner RW, Meyers DER, Richardson TL & Barker JL (1991). The site for initiation of action potential discharge over the somatodendritic axis of rat hippocampal CA1 pyramidal neurons. *J Neurosci* **11**, 2270–2280.

- Valberg PA, Kavet R & Rafferty CN (1997). Can low-level 50/60 Hz electric and magnetic fields cause biological effects? *Radiat Res* **148**, 2–21.
- Walsh V & Cowey A (2000). Transcranial magnetic stimulation and cognitive neuroscience. *Nat Rev Neurosci* **1**, 73–79.
- Warman EN, Grill WM & Durand D (1992). Modeling the effects of electric fields on nerve fibers: Determination of excitation thresholds. *IEEE Trans Biomed Eng* **39**, 1244–1254.
- Wong RKS & Stewart M (1992). Different firing patterns generated in dendrites and somata of CA1 pyramidal neurons in guinea-pig hippocampus. *J Physiol* **457**, 675–687.

Acknowledgements

This work was supported by the Medical Research Council (J.F., J.G.R.J.), the National Grid plc (J.G.R.J.), the Ministry of Education, Culture, Sports, Science and Technology of Japan (No.11480241, H.M.), and the Strategic Promotion System for Brain Science of the Special Coordination Funds for Promoting Science and Technology at the Ministry of Education, Culture, Sports, Science and Technology of Japan (H.M.). We would like to thank Martin Vreugdenhil for his valuable contribution to the data analysis, and Warren M. Grill and Cameron C. McIntyre for very helpful discussions and comments on an earlier version of this manuscript.